A novel epileptic encephalopathy mutation in *KCNB1* disrupts Kv2.1 ion selectivity, expression, and localization

Isabelle Thiffault,[1] David J. Speca,[4] Daniel C. Austin,[5] Melanie M. Cobb,[4] Kenneth S. Eum,[5] Nicole P. Safina,[3] Lauren Grote,[3] Emily G. Farrow,[1] Neil Miller,[1] Sarah Soden,[1,3,7] Stephen F. Kingsmore,[1,2,3,7] James S. Trimmer,[4,5] Carol J. Saunders,[1,2,7] and Jon T. Sack[5,6]

[1]Center for Pediatric Genomic Medicine, [2]Department of Pathology and Laboratory Medicine, and [3]Department of Pediatrics, Children's Mercy Hospital, Kansas City, MO 64108
[4]Department of Neurobiology, Physiology and Behavior, [5]Department of Physiology and Membrane Biology, and [6]Department of Anesthesiology and Pain Medicine, University of California, Davis, Davis, CA 95616
[7]University of Missouri—Kansas City School of Medicine, Kansas City, MO 64108

The epileptic encephalopathies are a group of highly heterogeneous genetic disorders. The majority of disease-causing mutations alter genes encoding voltage-gated ion channels, neurotransmitter receptors, or synaptic proteins. We have identified a novel de novo pathogenic K^+ channel variant in an idiopathic epileptic encephalopathy family. Here, we report the effects of this mutation on channel function and heterologous expression in cell lines. We present a case report of infantile epileptic encephalopathy in a young girl, and trio-exome sequencing to determine the genetic etiology of her disorder. The patient was heterozygous for a de novo missense variant in the coding region of the KCNB1 gene, c.1133T>C. The variant encodes a V378A mutation in the α subunit of the Kv2.1 voltage-gated K^+ channel, which is expressed at high levels in central neurons and is an important regulator of neuronal excitability. We found that expression of the V378A variant results in voltage-activated currents that are sensitive to the selective Kv2 channel blocker guangxitoxin-1E. These voltage-activated Kv2.1 V378A currents were nonselective among monovalent cations. Striking cell background–dependent differences in expression and subcellular localization of the V378A mutation were observed in heterologous cells. Further, coexpression of V378A subunits and wild-type Kv2.1 subunits reciprocally affects their respective trafficking characteristics. A recent study reported epileptic encephalopathy-linked missense variants that render Kv2.1 a tonically activated, nonselective cation channel that is not voltage activated. Our findings strengthen the correlation between mutations that result in loss of Kv2.1 ion selectivity and development of epileptic encephalopathy. However, the strong voltage sensitivity of currents from the V378A mutant indicates that the loss of voltage-sensitive gating seen in all other reported disease mutants is not required for an epileptic encephalopathy phenotype. In addition to electrophysiological differences, we suggest that defects in expression and subcellular localization of Kv2.1 V378A channels could contribute to the pathophysiology of this KCNB1 variant.

INTRODUCTION

The early infantile epileptic encephalopathies (EIEEs) are a group of disorders characterized by intractable seizures, persistently abnormal cortical function, and unfavorable neurodevelopmental outcomes (Berg et al., 2010; Nabbout and Dulac, 2012; Covanis, 2014). The etiologies include structural brain malformations, acquired brain insults, and inborn errors of metabolism (Nabbout and Dulac, 2012; Covanis, 2014). A significant proportion of these cases remain without molecular diagnosis despite extensive investigation. Recently, variants in genes encoding voltage-gated potassium (Kv) channels, including *KCNQ2* (Singh et al., 1998; Weckhuysen et al., 2013), *KCNQ3* (Cavaretta et al., 2014), and *KCNB1* (Srivastava et al., 2014; Torkamani et al., 2014), have been associated with EIEE (Maljevic and Lerche, 2014). *KCNB1* encodes the Kv2.1 pore-forming and voltage-sensing α subunit of a delayed rectifier Kv channel that is expressed in diverse neuron types (Trimmer, 2015). Kv2.1 is highly expressed in the neurons throughout the brain and forms the principal delayed rectifier current of many neuron types (Murakoshi and Trimmer, 1999; Du et al., 2000; Malin and Nerbonne, 2002; Guan et al., 2007; Mandikian et al., 2014). Kv2.1 plays important roles in regulating neuronal excitability, contributing to action potential repolarization (Liu and Bean, 2014) and dynamic modulation of neuronal activity (Misonou et al., 2004, 2008; Fox et al., 2013). In addition to its electrical roles in neurons, Kv2.1 plays a less understood structural role in neurons. Kv2.1 channels

Correspondence to Jon T. Sack: jsack@ucdavis.edu; James S. Trimmer: jtrimmer@ucdavis.edu; or Carol J. Saunders: csaunders@cmh.edu

Dr. Eum died on 22 June 2014.

Abbreviations used in this paper: EIEE, early infantile epileptic encephalopathy; GxTX, guangxitoxin-1E; Kv, voltage-gated potassium.

The Rockefeller University Press $30.00
J. Gen. Physiol. Vol. 146 No. 5 399–410
www.jgp.org/cgi/doi/10.1085/jgp.201511444

form large clusters on the cell body, proximal dendrites, and axon initial segments of neurons that represent plasma membrane–ER junctions (Trimmer, 1991; Antonucci et al., 2001; King et al., 2014; Fox et al., 2015). The majority of these clustered channels are reported to be nonconducting (O'Connell et al., 2010; Fox et al., 2013). The presence of Kv2.1 drives recruitment of other proteins to these clusters, indicating that subcellular localization of Kv2.1 could have neurophysiological consequences beyond electrical signaling (Antonucci et al., 2001; Fox et al., 2015).

Genetic defects in Kv2.1 lead to neurological consequences. Mice lacking Kv2.1 are strikingly hyperactive, defective in spatial learning, hypersensitive to convulsants, and exhibit accelerated seizure progression (Speca et al., 2014). Human genetic evidence indicates that mutations in Kv2.1 can lead to EIEE. De novo missense variants in *KCNB1* were initially reported in three patients with EIEE with associated cognitive and motor dysfunction (Torkamani et al., 2014). These variants were located within the Kv2.1 pore domain and associated with a loss of ion selectivity and voltage-sensitive gating, resulting in a tonic inward cation conductance. A fourth patient was recently identified through whole-exome sequencing (Srivastava et al., 2014). In this Communication, we report the fifth patient with a novel de novo variant in the *KCNB1* gene, c.1133T>C (p.V378A), located in the Kv2.1 pore domain, and a basic characterization of the effects of the mutation on channel expression and function. As this is the original reporting of this *KCNB1* variant, we present a clinical history of the patient. We then present functional evidence regarding the unique electrophysiological activity and subcellular localization of this Kv2.1 channel variant that could provide additional insight into the pathophysiological molecular mechanisms underlying the neurological defects seen in EIEE patients.

MATERIALS AND METHODS

Clinical reporting

Presentation of patient information, clinical findings, diagnostic assessment, therapeutic intervention, and outcomes conform to standardized clinical case report guidelines (Gagnier et al., 2013). All human studies were approved by the institutional review board of the Children's Mercy Hospital, and the parents gave informed consent for participation in the study.

Genetic analysis

DNA was extracted from peripheral blood of patient CMH574 and her two healthy parents (CMH575 and CMH576) and prepared with the Nextera Expanded Exome kit (Illumina). Samples were sequenced on a HiSeq 2000 instrument with TruSeq SBS v3 reagents (Illumina), yielding paired 100 nucleotide reads. Alignment, variant calling, and analysis were performed as reported previously (Bell et al., 2011; Saunders et al., 2012). Patient CMH574 was sequenced to a depth of 10.4 gigabases resulting in median target coverage of 135×, which identified ∼170,000 nucleotide variants. Variants were filtered to 1% minor allele frequency in an internal database of 2,129 samples, and then prioritized by the American College of Medical Genetics categorization (Richards et al., 2008), OMIM identity, and phenotypic assessment. The patient was found to have a heterozygous missense variant in exon 2 of *KCNB1*, c.1133T>C (p.V378A). The variant was confirmed by Sanger sequencing. Family relationships were confirmed by segregation analysis of rare single-nucleotide variants on several chromosomal regions. The *KCNB1* variant was absent from the patient's parents, the NHLBI Exome Sequencing Project, and an internal variant database.

Plasmids

A single T1133C point mutation was introduced into the hKv2.1/pRC/CMV plasmid (Zhang et al., 2003) encoding human Kv2.1 (RefSeq accession no. NP_004966) to generate the V378A plasmid. The modification was confirmed by sequencing. Where noted, an empty RBG4 plasmid was cotransfected to normalize total amount of DNA/transfection, or an empty EGFP-C1 plasmid (no. 6084-1; Takara Bio Inc.) was cotransfected to provide GFP expression in transfected cells. Kv2.1 ΔC237 was a previously described variant of rat Kv2.1 (Lim et al., 2000) in the pCGN plasmid (Tanaka and Herr, 1990). Human wild-type and V378A mutant plasmid DNA used in all experiments was transformed and purified identically and contemporaneously using a Maxiprep purification kit (QIAGEN).

Cell culture and transfection

All cell lines were grown in a humidified incubator at 37°C and 5% CO_2. COS-1 cells were maintained in Dulbecco's modified Eagle's medium supplemented with 10% bovine calf serum (HyClone), 1% penicillin/streptomycin, and 1× GlutaMAX (Thermo Fisher Scientific). COS-1 cells were split to 10% confluence and then transfected in Opti-MEM (Thermo Fisher Scientific) 24 h later with the constructs described above using LipofectAMINE 2000 (Thermo Fisher Scientific) according to the manufacturer's protocol. Media was replaced 4 h after transfection. COS-1 cells were used 40–48 h after transfection. CHO-K1 (CCL-61; ATCC) cells were maintained in tissue culture–treated polystyrene dishes (BioLite; Thermo Fisher Scientific), Ham's F12 media (MT-10-080-CV; Corning) containing 10% FBS (GemCell), and 1% penicillin/streptomycin (Thermo Fisher Scientific). Cells were transfected in Ham's F12 media with LipofectAMINE 2000 according to the manufacturer's protocol, using 2 µl Lipofectamine, and 1 µg DNA per milliliter media. Media was replaced 4–6 h after transfection, and cells were used for experiments 2 d later.

Electrophysiology

Whole-cell voltage-clamp recordings were used to measure currents from Kv2.1 channels expressed in CHO-K1 cells. Cells were harvested by scraping in divalent-free PBS with 1 mM EDTA, pelleted at 650 *g* for 7 min, resuspended in CHO-SFMII media (Thermo Fisher Scientific) supplemented with 25 mM HEPES, pH 7.3, and rotated in a polypropylene tube at room temperature until use. Aliquots of cell suspension were added to a recording chamber and rinsed with external solution 5 or more minutes before recording. The external (bath) solution contained (mM): 3.5 KCl, 155 NaCl, 1.5 $CaCl_2$, 1 $MgCl_2$, and 10 HEPES, adjusted to pH 7.4 with NaOH. The internal (pipet) solution contained (mM): 50 KF, 70 KCl, 35 KOH, 5 EGTA, and 50 HEPES, adjusted to pH 7.3 with HCl. A measured liquid junction potential of 12 mV was corrected. The Kv2 inhibitor GxTX is the guangxitoxin-1E toxin with methionine 35 replaced by norleucine, synthesized as described previously (Tilley et al., 2014). GxTX was added by flushing 200 µl through a low volume recording chamber (R-24N;

Warner). Pipettes were pulled from thin-wall borosilicate glass (no. BF150-110-7.5HP; Sutter Instrument). Pipette tip resistances were <3 MΩ. Recordings were performed at room temperature (21–23°C). Voltage clamp was achieved with an amplifier (Axon Axopatch 200B; Molecular Devices) run by Patchmaster software (HEKA). The holding potential was −100 mV. Series resistance compensation was used when needed to constrain voltage error to <10 mV. Capacitance and ohmic leak were subtracted using a P/5 protocol. Recordings were low-pass filtered at 10 kHz and digitized at 100 kHz. Current traces were digitally filtered at 2 kHz for display in figures. Data were analyzed and plotted with IgorPro software (Version 6; WaveMetrics). Conductance was measured from tail currents immediately after a 100-ms step to the indicated voltage; tails were analyzed at 0 mV for wild-type channels and at −100 mV for V378A. Fits with the fourth power of a Boltzmann distribution are described previously (Sack et al., 2004; Tilley et al., 2014). Conductance data shown are normalized to the peak amplitude of the fit; V_{mid} reported is the voltage when the fit reaches half-maximal amplitude. Ion selectivity experiments were conducted by exchange of external solution. 155 mM NaCl was replaced by RbCl, CsCl, KCl, NH_4Cl, or NMDG + HCl, and adjusting pH to 7.4 with NMDG. Ionic permeability was calculated from the reversal potential with the indicated ion in the external solution, as described previously (Heginbotham et al., 1994). The ratio P_X/P_K is the permeability of the indicated ion normalized to K^+.

Immunofluorescence immunocytochemistry

COS-1 and CHO-K1 cells grown on poly-L-lysine–coated glass coverslips were fixed for 15 min in ice-cold 4% formaldehyde prepared fresh from paraformaldehyde, 4% sucrose, and 0.1% Triton X-100 in DPBS (137 mM NaCl, 2.7 mM KCl, 10 mM Na_2HPO_4, and 1.76 mM KH_2PO_4, pH 7.4) with 1 mM $CaCl_2$ and 1 mM $MgCl_2$, or were fixed for 30 min in 4% formaldehyde prepared fresh from paraformaldehyde and 4% sucrose in DPBS. Cells were blocked and permeabilized with 3% (wt/vol) bovine serum albumin and 0.1% Triton X-100 in DPBS for 60 min, and then coverslips were incubated with primary antibody overnight at 4°C (anti-Kv2.1 K89/34 IgG1: 1:20 dilution of tissue culture supernatant, Research Resource Identifier [RRID]: AB_10672253; anti-GFP N86/38 IgG2a: 1:5 dilution of tissue culture supernatant, RRID: AB_10671955; both from the UC Davis/National Institutes of Health [NIH] NeuroMab Facility; anti-HA, RRID: AB_2532070). Primary antibodies were detected with appropriate mouse IgG subclass-specific fluorescent secondary antibodies (A21127, A21131, A21121, and A21147; 1:2,000; Thermo Fisher Scientific) and Hoechst 33258 stain (H21491; Thermo Fisher Scientific). Coverslips were washed again in DPBS and mounted using Prolong Gold (P36930; Thermo Fisher Scientific). Images were acquired using an AxioCam HRm high resolution CCD camera installed on an AxioObserver Z1 microscope with a 63×, 1.3-numerical aperture (NA) lens or a 20×, 0.8-NA lens and an Apotome controlled by Axiovision software (Carl Zeiss). Images were processed identically in Photoshop to maintain consistency between samples.

Immunoblots

Cell lysates were prepared as described previously (Shi et al., 1994). Proteins were separated by 9% SDS-PAGE and transferred to nitrocellulose membranes. Blots were probed with rabbit anti-Kv2.1 (1:500; KC; RRID: AB_2315767) and as loading controls mouse anti-mortalin (1:2, N52A/42 tissue culture supernatant; RRID: AB_10674108, from the UC Davis/NIH NeuroMab Facility) or rabbit anti-actin (1.0 µg/ml; RRID: AB_630834; sc-1616R; Santa Cruz Biotechnology, Inc.) for 60 min in TBS, followed by incubation with appropriate fluorescently labeled secondary antibody (1:1,500) for an additional 60 min. Imaging and quantitation of blots was performed on a FluorChem Q imager (Protein Simple), using the multiplex band analysis tool (version 3.4.0) to assess Kv2.1 fluorescence intensity after background subtraction. Kv2.1 expression intensity was then normalized to either the actin or mortalin-loading control for each sample before statistical analysis.

Analysis and statistics

GraphPad Prism (version 6.0b) or IgorPro (version 6; WaveMetrics) software was used for presentation and statistical analyses of microscopy or electrophysiology data, respectively. Data are presented as means ± SEM.

Accession numbers

The RefSeq accession numbers for *KCNB1* variants reported in this paper are NM_004975.2 and NP_004966.1.

RESULTS

Clinical data

A 3-yr-old Caucasian female presented with intractable multifocal epilepsy, global developmental delay, and difficulty feeding. Prenatal history was unremarkable; delivery was at full-term with a normal neonatal period. Her first recognized seizure at 13 mo lasted for ∼10 min. EEG recordings revealed intermittent left and right temporal/temporal parietal spike, polyspike and slow wave discharges, and intermittent superimposed left and right temporal focal slowing. Starting in the first months of life, she was easily startled, blinked repeatedly, and had episodes of staring, suggesting an earlier onset of seizures. Brain MRI at 13 and 18 mo were normal.

She developed a social smile at age 3 mo and rolled between 6 and 10 mo of life. Between 13 and 15 mo, she began to regress significantly in skills and developed oral motor dysphagia requiring liquid formula supplementation. At 15 mo, she was able to sit with some support, and by age 3 yr she was able to sit independently but could not stand or walk. She never developed speech, only limited vocalization and inappropriate laughter. At age 3 yr she functioned at a 5–8-mo developmental level. Her seizures were refractory to numerous medications including Keppra, Depakote, Clobazam, Zonisamide, and Lamictal. After implementation of the ketogenic diet, she was initially seizure free for 6 mo, followed by breakthrough seizures ranging from 1 to >20 per day. Relevant family history included febrile seizures in the patient's mother until age 9. An extensive workup was normal, including: high resolution karyotype, CGH microarray, methylation studies for Angelman syndrome, palmitoyl protein thioesterase 1 and tripeptidyl peptidase 1 enzymes, comprehensive epilepsy gene panel (53 genes; no. 523; GeneDX), sequence and deletion/duplication analysis, carbohydrate-deficient transferrin analysis, N-glycan structural analysis, very long chain fatty acids, plasma amino acids, 7-dehydrocholesterol, urine organic acids, and oligosaccharides.

Whole-exome sequencing analyses reveal a novel de novo KCNB1 missense variant

The patient was found to be heterozygous for a de novo missense variant, 1133T>C, in exon 2 of *KCNB1*, which encodes the Kv2.1 channel. This variant affects codon 378, a highly conserved amino acid residue in the pore helix of the Kv2.1 channel. The mutation substitutes valine 378 with alanine, the disruption of which is predicted by SIFT (Kumar et al., 2009) and PolyPhen2 (Adzhubei et al., 2010) to be damaging. Valine 378 is the amino acid position just before the "GYG" motif, encoded by residues 379–381, which defines the K^+ selectivity filter. Previous studies found that a valine to alanine mutation at the equivalent residue in the *Drosophila melanogaster* Shaker Kv channel results in voltage-activated channels exhibiting loss of ion selectivity (Heginbotham et al., 1994), suggesting that degenerate ion permissiveness may underlie the functional defect in our patient.

Kv2.1 V378A forms voltage-activated ion channels

To determine whether the V378A variant alters the function of the Kv2.1 channel, we expressed wild-type and mutant human Kv2.1 channels in CHO-K1 cells and examined whole-cell current under voltage clamp. Cotransfection of the wild-type Kv2.1 construct with a GFP construct resulted in voltage-activated currents in green fluorescent cells (GFP+). When voltage was stepped positive from a negative holding potential, outward currents resulted after a delay, with a sigmoid waveform (Fig. 1 A) indicative of the human voltage-activated delayed rectifier Kv2.1 channel (Ikeda et al., 1992; Zhang et al., 2003; Torkamani et al., 2014). Transfections of the V378A construct also resulted in voltage-activated currents (Fig. 1 B). These currents are distinct from the previously described EIEE-linked *KCNB1* variants, S347R, G379R and T374I, none of which retained voltage activation (Torkamani et al., 2014). After a positive voltage step, the outward currents from V378A exhibited a marked peak followed by decay, indicating that inactivation occurs at a faster rate in the mutant channels; upon return to the negative holding voltage, V378A displayed larger inward tail currents (Fig. 1, A and B). The voltage dependence of channel gating was reconstructed from tail currents after depolarizing voltage stimuli (Fig. 1 C). This analysis indicated that voltage-dependent gating of the V378A variant was distinct from wild type yet had a similar steepness when fitted with a Boltzmann distribution. The incidence of voltage-activated current in GFP+ cells was low compared with wild-type Kv2.1; voltage-activated currents >400 pA at 60 mV were apparent in only 20% (18/88) of V378A GFP+ cells recorded, compared with 68% (38/56) for cells transfected with wild-type Kv2.1. As endogenous voltage-gated currents can occasionally be present in CHO-K1 cells (Lalik et al., 1993), we tested whether the currents from V378A-transfected cells had pharmacology typical of Kv2.1 channels. The tarantula venom peptide toxin GxTX is the most thoroughly validated Kv2.1 inhibitor (Herrington et al., 2006; Li et al., 2013; Liu and Bean, 2014) and does not bind to CHO-K1 cells lacking Kv2.1 channels (Tilley et al., 2014). Currents from both wild-type Kv2.1 and V378A cells were inhibited by GxTX (Fig. 1, D–F), corroborating the conclusion that the voltage-activated currents with large inward tail currents originated from Kv2.1 channels.

Kv2.1 V378A channels are not K^+ selective

The reversal potential of Kv2.1 was notably altered by the V378A variant. Distinct from wild-type Kv2.1 channels, V378A channels produced large inward tail currents at voltages much more positive than the calculated K^+ reversal potential of −97 mV (Fig. 2, A and B), suggesting that ions other than K^+, such as Na^+, might permeate the mutant channels. To test this hypothesis, we

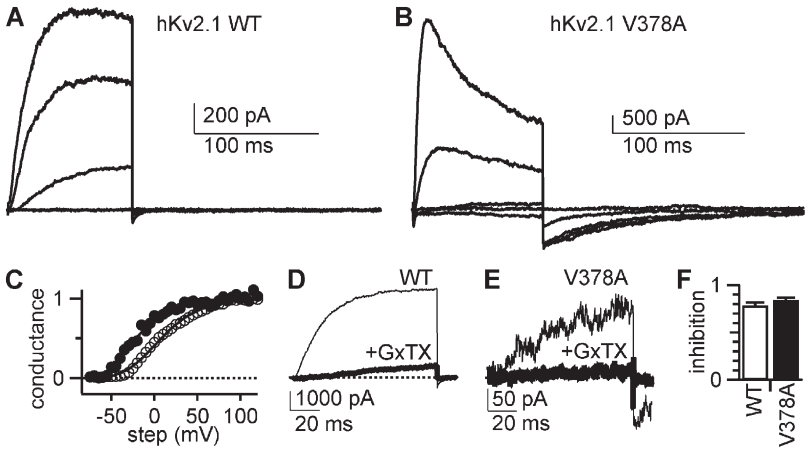

Figure 1. The Kv2.1 V378A mutant produces voltage-activated currents. Whole-cell patch-clamp recordings from transiently transfected CHO-K1 cells. Currents are responses to voltage steps from a holding potential of −100 mV. (A) Kv2.1 wild-type currents were stepped for 100 ms to −80, −40, 0, 40, or 80 mV, and then returned to −100 mV. (B) Kv2.1 V378A currents elicited by the same protocol as A. (C) Conductance–voltage relation of Kv2.1 wild-type (open circles) and V378A (filled circles) measured from tail currents after 100-ms depolarizing steps to the indicated voltage. Lines are fourth-power Boltzmann fits. Wild-type V_{mid} = 8 mV and z = 0.9 e^+; V378A V_{mid} = −21 mV and z = 1.1 e^+. (D) Current from wild-type Kv2.1. 100-ms step to 40 mV. Thin trace, control; thick trace, 100 nM GxTX. (E) Kv2.1 V378A currents, with same protocols as D. (F) Summary of inhibition by 100 nM GxTX at 40 mV. Wild-type, n = 4; V378A, n = 3. Error bars represent means ± SEM.

substituted extracellular sodium with $NMDG^+$, a large cation that cannot permeate most ion channels. $NMDG^+$ substitution reduced the large inward tail currents. This indicates that Na^+ was indeed permeating the V378A channel (Fig. 2, B, D, and E). To test if the V378A channel had completely lost the ability to select between monovalent cations, we measured the relative permeabilities of K^+, Na^+, $NMDG^+$, Rb^+, Cs^+, and NH_4^+. Significantly greater permeability was seen for Na^+, Cs^+, and NH_4^+ (Fig. 2 F). None of the metal ions had a permeability distinguishable from K^+. This is similar to the effects of the homologous mutation in the *Shaker* K^+ channel (V443A) (Heginbotham et al., 1994). The loss of ionic selectivity suggests that in vivo, voltage activation of Kv2.1 V378A channels would result in Na^+ flux through the channel along with K^+, eliminating the ability of the channel to repolarize cells. Instead, Kv2.1 V378A would likely depolarize cells upon channel opening.

To generate a channel expression profile that could better mimic the EIEE patient heterozygous for Kv2.1 V378A, we cotransfected equal amounts of Kv2.1 wild-type and V378A subunits. The proportion of cotransfected cells with distinct delayed rectifier current (34/78 of GFP+ cells, 44%, had voltage-activated currents >400 pA at 60 mV) was intermediate between those seen upon expression of wild-type Kv2.1 and V378A subunits alone (see above). However, the voltage-activated currents recorded from V378A/wild-type Kv2.1 cotransfections had ionic selectivity similar to wild-type Kv2.1 (Fig. 2 F). This suggests that currents through channels containing V378A subunits could be small relative to channels containing only wild-type subunits, and/or that heteromeric wild-type/mutant channels may not localize efficiently to the plasma membrane.

The V378A mutation alters Kv2.1 expression

The changes in function of the V378A mutant channel potentially underlie the human disease phenotype, as proposed for other Kv2.1 pore mutations (Torkamani et al., 2014). However, it was notable that V378A channels failed to produce significant current in the majority of patch-clamped cells, suggesting an alteration in protein expression or localization. Expression and localization of wild-type and V378A channels were tested by immunofluorescence labeling of transfected cells with specific anti-Kv2.1 antibodies. CHO-K1 cells were transiently cotransfected with GFP and wild-type Kv2.1 or V378A. Multiplex immunofluorescence labeling (Fig. 3 A) indicated that although the incidence of GFP expression was similar between cultures transfected with wild-type and V378A plasmids, fewer cells expressed V378A protein relative to wild-type Kv2.1. Specifically, although GFP was expressed in ∼20% of cells cotransfected with either Kv2.1 wild-type or V378A plasmids, detectable

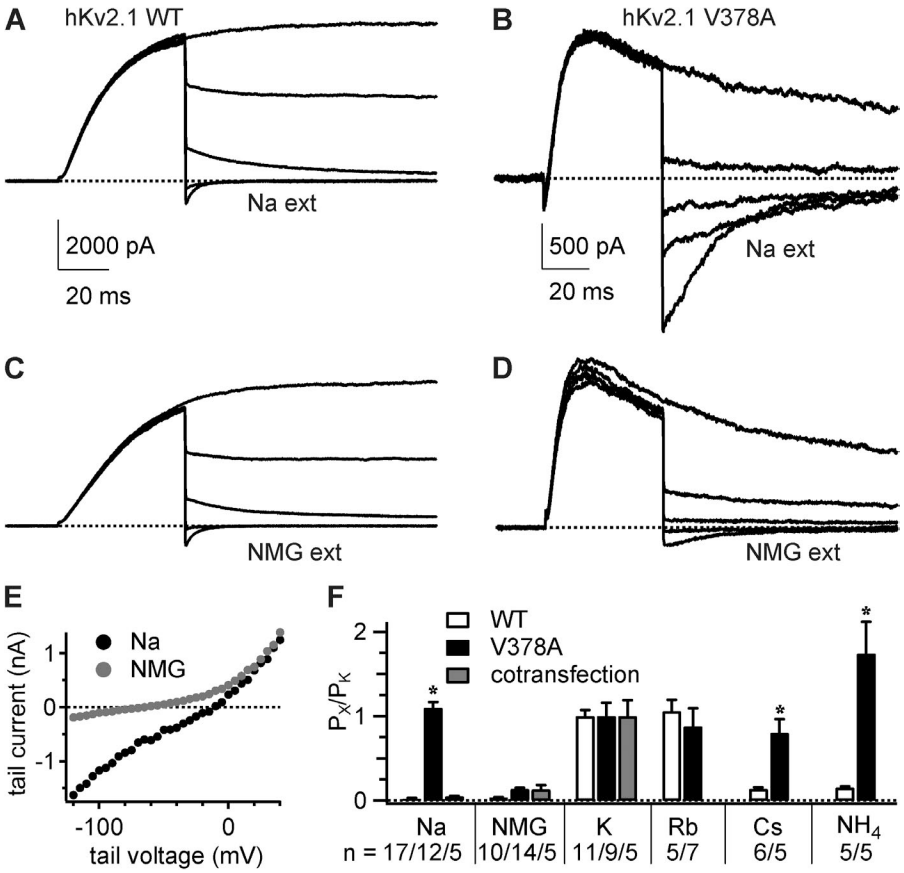

Figure 2. The Kv2.1 V378A mutant is a nonselective cation channel. Whole-cell patch-clamp recordings from transiently transfected CHO-K1 cells. Currents are responses to voltage steps from a holding potential of −100 mV. (A) Kv2.1 wild-type currents. 50-ms steps to 40 mV, and then to −120, −80, −40, 0, or 40 mV. (B) Kv2.1 V378A currents elicited by the same protocol as A. (C and D) Same cell and protocol as in A and B but with external Na^+ replaced by $NMDG^+$. (E) Instantaneous current level from Kv2.1 V378A at the indicated voltage after a 50-ms step to 40 mV in control external (black) or NMDG external (gray). (F) Permeability ratios for the indicated ion over K^+, calculated from the reversal potential when external Na^+ is replaced with the indicated ion. Cotransfection delivered an equal amount of wild-type and V378A DNA. *, $P < 0.01$, compared with wild type by two-tailed Mann–Whitney *U* test. Error bars represent means ± SEM.

immunolabeling for V378A protein was found in a significantly lower percentage (1.6%) of cells than wild-type Kv2.1 (7.2%; Fig. 3 B). Thus, the incidence of Kv2.1 protein expression and voltage-activated current (see above) were both reduced by the V378A mutation. Notably, there were no obvious differences in localization of the V378A protein relative to wild-type Kv2.1 in CHO-K1 cells (Fig. 3 A). Immunoblot analysis also indicated that total levels of V378A protein were lower than wild-type Kv2.1 (Fig. 3, C and D). Sodium influx can be toxic to cells, potentially reducing protein expression. To test whether reduced V378A expression is a response to permeation through the nonselective channels, transfected CHO-K1 cells were cultured in the presence of GxTX, which inhibits ion flux through both Kv2.1 wild-type and V378A (Fig. 1 F). However, GxTX treatment failed to rescue the reduced expression level of the V378A mutant in CHO-K1 cells, as assayed by immunoblot (Fig. 3, C and D).

To test whether the reduced expression of V378A channels seen in CHO-K1 cells was a generalized phenomenon, we examined the expression of V378A in another mammalian cell type, COS-1, in which we have extensively characterized the subcellular localization of rat Kv2.1 (e.g., Shi et al., 1994). Significant differences were also observed in Kv2.1 expression incidence between wild-type and V378A mutant Kv2.1 in COS-1 cells, although the fractional decrement with V378A was not as profound as in CHO-K1 cells (Fig. 4 A). No significant decrement in expression incidence was observed when wild-type and V378A subunits were coexpressed (Fig. 4 A). The subcellular localization of the V378A mutant was distinct from wild-type Kv2.1 in COS-1 cells. Wild-type Kv2.1 was observed at/near the plasma membrane, as described previously for rat Kv2.1 in this cell type (Shi et al., 1994). This plasma membrane pattern was observed only in a subset of cells expressing V378A, as a significant fraction of cells exhibited little to no expression at/near the plasma membrane (Fig. 4 B). Remarkably, incubation of COS-1 cells with GxTX rescued the expression pattern of the V378A mutant, changing the localization to a plasma membrane–like pattern more typical of wild-type Kv2.1 (Fig. 4, B and C). V378A-expressing cells with no plasma membrane–associated labeling exhibited robust intracellular immunofluorescence labeling that overlapped with *Lens culinaris* lectin labeling, a marker of the Golgi apparatus (Hsu et al., 1992; Ridgway et al., 1992; Fig. 4 D). Immunoblot analyses of COS-1 cells revealed lower levels of the V378A mutant protein, similar to what was observed in CHO-K1 cells (Fig. 3, C and D). Consistent with effects observed by immunofluorescence labeling, effects of treatment with GxTX could also be seen by immunoblotting of COS-1 cells, which showed that the reduced level of V378A protein expression was restored to that of wild-type Kv2.1 upon GxTX treatment (Fig. 4, E and F).

The distinct differences in subcellular localization of the mutant and wild-type Kv2.1 isoforms raised questions as to the effects of their coexpression, as occurs in

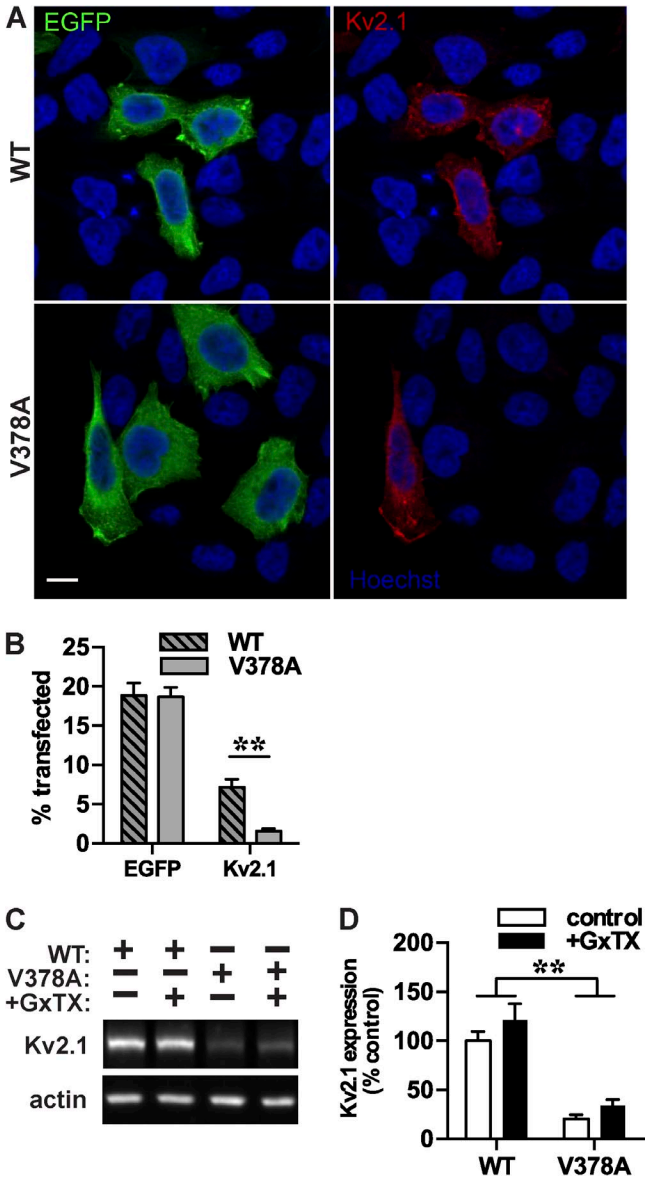

Figure 3. Decreased Kv2.1 V378A expression and lack of rescue by GxTX in CHO-K1 cells. (A) Multiplex imaging of EGFP (green), Kv2.1 (red), and Hoechst 33258 (blue, to label nuclei), indicating reduced incidence of Kv2.1 V378A expression compared with wild-type Kv2.1. Bar, 10 µm. (B) Similar transfection efficiency of EGFP but significantly lower transfection efficiency of Kv2.1 V378A compared with wild-type Kv2.1, as measured by immunofluorescence labeling (n = 3 independent samples per treatment). (C) Immunoblot analysis of CHO-K1 cell extracts cultured in the absence or presence of 400 nM GxTX, showing reduced levels of V378A Kv2.1 protein that is not rescued by 400 nM GxTX treatment. Actin was used as a loading control. (D) Quantitation of immunoblot analyses demonstrating significantly lower expression and lack of GxTX rescue in Kv2.1 V378A-expressing cells relative to wild type (n = 3 per treatment). **, $P < 0.01$, by two-way ANOVA followed by post-hoc Tukey tests. Error bars represent means ± SEM.

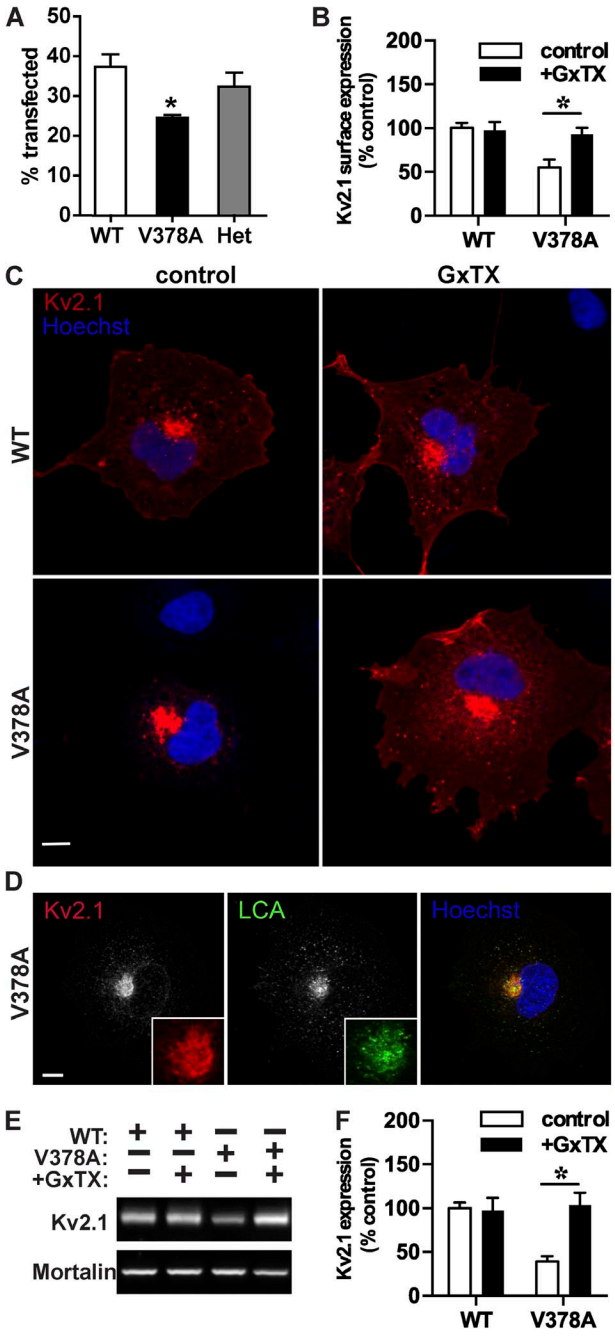

heterozygous patients. To test how expression of mutant V378A subunits could impact the surface localization of wild-type subunits, and vice versa, we exploited an epitope-tagged Kv2.1 C-terminal truncation mutant ΔC237, which is wild type throughout, including at the pore region, and has a subcellular localization indistinguishable from wild-type Kv2.1 (Lim et al., 2000) but lacks immunoreactivity with the anti-Kv2.1 antibody used here to detect the expression of the V378A mutant. The wild-type Kv2.1 ΔC237 truncation mutant was coexpressed with human Kv2.1 V378A. Immunolabeling for antibodies that selectively recognize one or the other allowed us to separately determine the subcellular localization of the wild-type and mutant Kv2.1 subunits in coexpressing cells. Coexpression revealed a reciprocal effect of wild-type and mutant subunits on subcellular localization, in that each was impacted by the presence of the other. Specifically, a prominent decrease in plasma membrane–associated immunolabeling for ΔC237, and an increased intracellular retention, was observed upon its coexpression with V378A. Moreover, coexpression of ΔC237 with the V378A mutant yielded an increase in V378A plasma membrane–associated immunolabeling (Fig. 5 A). At the individual cell level, the distinct subcellular localizations of ΔC237 with the V378A seen in singly expressing cells became more similar upon coexpression, with substantial overlap of immunolabeling for both isoforms in both intracellular and plasma membrane compartments (Fig. 5 B).

DISCUSSION

Trio-exome sequencing has become an effective tool for EIEE diagnosis, with de novo variants in ion channels playing a prominent role (Weckhuysen et al., 2013; EuroEPINOMICS-RES, 2014; Dyment et al., 2015). Consistent with their extreme genomic, proteomic, and functional diversity, Kv channels have been implicated in an exceptionally wide variety of genetic and autoimmune neurological disorders, including episodic ataxia,

Figure 4. Altered subcellular localization and rescue of expression of Kv2.1 V378A in COS-1 cells. (A) Transfection efficiency of wild-type, V378A, and an equal amount of wild-type + V378A (Het) in COS-1 cells, as measured by immunofluorescence. Data are from at least 115 cells per independent sample ($n = 3$ for each treatment). Data are the mean ± SEM. *, $P < 0.05$ (two-tailed unpaired t test). (B) Quantitation of surface expression of Kv2.1 in the absence or presence of 400 nM GxTX ($n = 3$ per treatment). (C) Multiplex fluorescence labeling for Kv2.1 (red) and Hoechst 33258 (blue) in cells cultured in the absence or presence of 400 nM GxTX. Wild-type Kv2.1 expression was robust and associated with the plasma membrane regardless of treatment. In contrast, V378A expression was, in a significant fraction of cells, restricted to an intracellular perinuclear compartment consistent with the Golgi apparatus, whereas V378A cells cultured in the presence of 400 nM GxTX had more plasma membrane–associated labeling, resembling that of wild-type Kv2.1. Bar, 10 µm. (D) Multiplex fluorescence labeling of a Kv2.1 V378A-expressing cell for Kv2.1 (red), the Golgi marker *Lens culinaris* lectin (green), and Hoechst 33258 (blue, to label nuclei) suggests a concentration of Kv2.1 V378A in the Golgi apparatus. Insets are a higher magnification of the perinuclear region. Bar, 10 µm. (E) Immunoblot analysis of COS-1 cell extracts cultured in the absence or presence of 400 nM GxTX, showing reduced levels of V378A mutant Kv2.1 protein that is rescued by GxTX. Mortalin was used as a loading control. (F) Quantitation of Kv2.1 immunoblot expression normalized to the mortalin loading control indicates a significantly decreased level of expression of Kv2.1 V378A relative to wild-type Kv2.1. Culturing cells in the presence of 400 nM GxTX rescues the decreased V378A expression level in this cell type ($n = 3$ per treatment). *, $P < 0.05$, by two-way ANOVA followed by post-hoc Tukey tests.

periodic paralysis, benign familial neonatal seizures, peripheral nerve hyperexcitability, and EIEEs (Maljevic and Lerche, 2014). As human genetic data accumulates, general mechanistic origins of epileptic Kv channelopathies may begin to emerge.

Similar to *KCNB1*, multiple *KCNQ2* (Kv7.2) mutations have been found to be causative of EIEE (Dedek et al., 2003; Weckhuysen et al., 2012). These two Kv channels have limited anatomical overlap in the brain. In central neurons, Kv7.2 is localized to axon initial segments and nodes of Ranvier where it mediates diverse aspects of axonal excitability (Devaux et al., 2004). Although the bulk of Kv2.1 is present in the plasma membrane of the soma and proximal dendrites, it is also expressed at high density on the axon initial segment in rodent and human brains (Sarmiere et al., 2008; King et al., 2014; Trimmer, 2015). The axon initial segment has high levels of Kv7.2 expression, and this neuronal subcellular compartment has been highlighted as a "hot spot" for epileptogenesis, as mutations of many ion channels found here (e.g., Nav1.1/*SCN1*A, Navβ1/*SCN1B*, Kv1.1/*KCNA1*, Kv7.2/*KCNQ2*, Kv7.3/*KCNQ3*, and GABA-A receptor γ2/*GABRG2*) give rise to epilepsy (Wimmer et al., 2010). Thus, Kv2.1/*KCNB1* joins this list of ion channels localized to the axon initial segment and associated with epilepsy-related mutations, raising the possibility that the epileptogenic effects of Kv2.1 mutation may arise from an electrical defect in the axon initial segment.

The de novo V378A variant in *KCNB1* fundamentally changes the ion selectivity of Kv2.1 channels from potassium-selective to nonselective cation channels, as was also demonstrated for three previously reported de novo *KCNB1* mutations (Torkamani et al., 2014). To date, all reported missense variants are located within the pore domain of Kv2.1 (Srivastava et al., 2014; Torkamani et al., 2014). All variants that have been studied in heterologous expression systems reported here and previously (Torkamani et al., 2014) have formed channels with loss of K^+ selectivity, yielding a depolarizing inward cation conductance at negative voltages. Notably, the variant we report here is functionally distinct from those whose currents have been reported previously, in that the V378A channel is gated by voltage, whereas the other disease-associated Kv2.1 mutations characterized to date remain constitutively open (Torkamani et al., 2014). V378A channels are voltage dependent and sensitive to the Kv2-specific toxin GxTX, providing compelling evidence that the nonselective cation currents recorded from cells expressing the mutant channels are from bona fide Kv2.1 channels. These findings support the previously proposed pathogenic role for altered ionic selectivity, yet suggest that the abrogation of voltage-activated gating reported for all other Kv2.1 EIEE mutations that have been studied by voltage clamp (Torkamani et al., 2014) is not required for a disease phenotype.

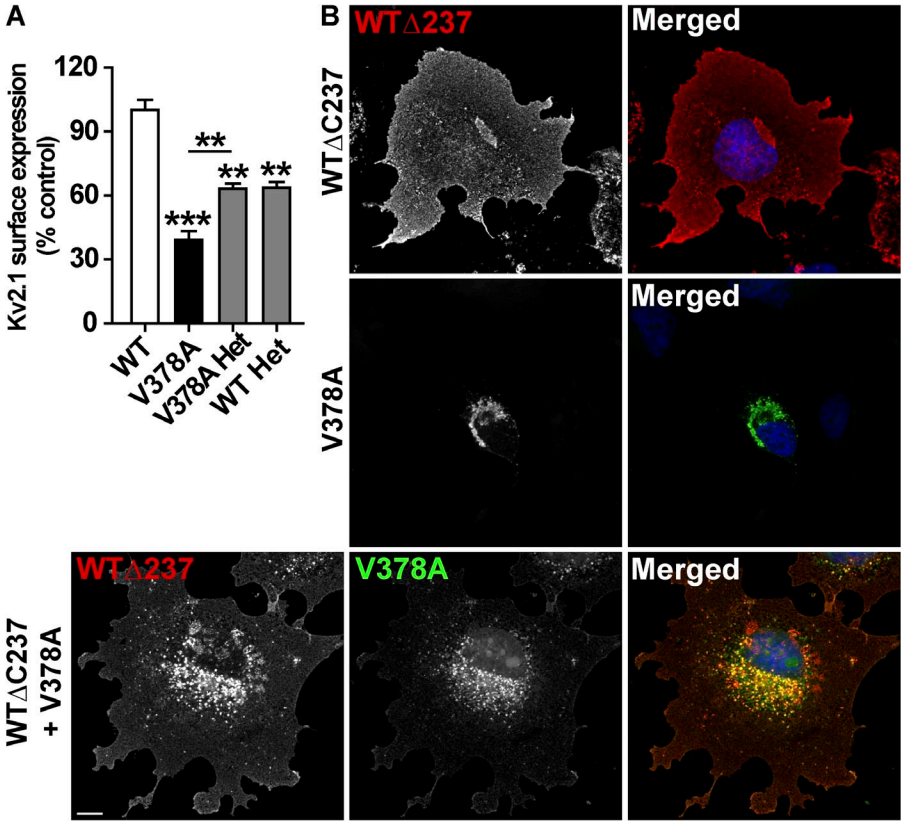

Figure 5. Coexpression of wild-type Kv2.1 ΔC237 and Kv2.1 V378A results in intermediate surface expression levels. (A) Cell surface expression of wild-type Kv2.1 ΔC237 (WT), Kv2.1 V378A (V378A), Kv2.1 V378A in the presence of wild-type Kv2.1 ΔC237 (V378A Het), and wild-type Kv2.1 ΔC237 in the presence of Kv2.1 V378A (WT Het) as determined by immunofluorescence in COS-1 cells, using antibodies that distinguish wild-type Kv2.1 ΔC237 and Kv2.1 V378A. Data are from at least 80 cells per independent sample (n = 3 per treatment). Data are the mean ± SEM. **, $P < 0.01$; ***, $P < 0.001$ (two-tailed unpaired t test). (B) Multiplex immunofluorescence labeling for wild-type Kv2.1 ΔC237 (red), Kv2.1 V378A (green), and Hoechst 33258 (blue) in cells expressing wild-type Kv2.1 ΔC237 alone (top), expressing Kv2.1 V378A alone (middle), or expressing both subunits (bottom). Images were acquired with optimal exposure. Bar, 10 µm for all panels.

In addition to altered ion selectivity, our immunocytochemistry experiments in transfected COS-1 cells reveal drastic changes in the subcellular localization of the human Kv2.1 V378A mutant, and a reduction of apparent transfection efficiency. This could be a cellular response to a toxic inward current through V378A that triggers channel internalization and cell death, as these phenotypes are partially rescued by culturing cells in the Kv2 inhibitor GxTX. Additionally, the changes in V378A channel conductance result from structural defects in the K^+ channel selectivity filter, which could impact the stability and localization of channel protein. Removal of K^+ ions from the K^+ channel pore leads to pore collapse (Zhou et al., 2001) and degradation of Kv channel proteins (Parcej and Dolly, 1989). Changes to the structure of the pore of Kv channels can also alter their trafficking (Manganas et al., 2001b; Vacher et al., 2007). Synonymous defects in pore structure and localization suggest caution in ascribing the pathophysiology of the Kv2.1 pore mutations to channel conductance without taking into consideration possible effects on channel expression and localization.

Exogenous alteration of ion channel function can also alter channel localization. Inhibitors of ion channels have been shown to lead to pharmacological rescue of their normal expression patterns. Kv1 channel expression can be rescued by peptide inhibitors (Vacher et al., 2007; Rangaraju et al., 2010), similar to the effects of GxTX on Kv2.1 V378A channels in COS-1 cells. Pharmacological rescue of expression has also been observed for several other disease-associated ion channel mutations, most prominently mutant CFTR and HERG (*KCNH2*) channels, which result in cystic fibrosis (Cai et al., 2011) and cardiac arrhythmias (Balijepalli et al., 2010), respectively. In these cases, pharmacological rescue has been primarily attributed to chaperone-like effects on biosynthetic folding of the mutant channels within the ER, leading to release from retention in the ER and cell surface expression (Leidenheimer and Ryder, 2014). A similar rescue of episodic ataxia-related Kv1.1 mutants is observed in response to treatment with general chemical chaperones (Manganas et al., 2001b), which are also presumed to act at the level of protein folding in the ER. These known mechanisms of rescue rely on treatments with membrane-permeable compounds that can access intracellular compartments such as the ER. The mechanism underlying the pharmacological rescue of the V378A mutants in COS-1 cells, and the lack of rescue by GxTX in CHO-K1 cells, is not known. However, that GxTX rescued V378A expression in COS-1 cells, which have a substantial intracellular (Golgi) pool of mutant channels, versus CHO-K1 cells, which do not, is consistent with such an intracellular mechanism of pharmacological rescue. GxTX partitions into the outer leaflet of cell membranes, where it binds to membrane-facing regions of Kv2 channels (Milescu et al., 2009; Gupta et al., 2015). Through an endocytotic mechanism, GxTX could potentially access intracellular membranes and mediate rescue of the Golgi-localized V378A mutant via chaperone-like effects on channel folding, as observed in the pharmacological and chemical rescue of other intracellularly retained disease-associated ion channel mutants. Alternately, GxTX could rescue expression of the V378A mutant by binding surface channels and preventing internalization, either by stabilizing their protein structure or by inhibiting their potentially toxic nonselective inward currents.

The patient described here is heterozygous for the de novo KCNB1 mutation that yields V378A Kv2.1. The distinct phenotypes of the V378A mutant, specifically alterations in both ion selectivity and subcellular localization, are somewhat mitigated by coexpression with Kv2.1 isoforms with wild-type properties. This suggests that the Kv2.1 phenotype of the heterozygous patient may not be as drastically altered as it would be in a homozygous phenotype, and that within the tetrameric Kv2.1 channels, the mutant V378A subunits may exert dose-dependent as opposed to dominant effects on wild-type subunits. Detailed analyses of Kv2.1 channels with distinct subunit stoichiometries, of the type needed to determine how the subunit stoichiometry yields the distinct phenotypes of tetrameric channels, have not been performed. This could be achieved through extensive dose–response studies of wild-type and mutant subunits to bias their respective assembly into heteromeric channels with a predominance of wild-type or mutant subunits within the channel population, and the subsequent deconvolution of the expressed channel characteristics to determine the details of the channels with distinct characteristics (Ruppersberg et al., 1990; MacKinnon, 1991; Manganas and Trimmer, 2000), or generation of concatenated subunits to generate tetrameric channels with covalently defined subunit compositions (Sack et al., 2008). Future studies may reveal the nature of the impact of the growing number of diverse *KCNB1* mutations associated with epileptic encephalopathies on heteromeric channels, as has been performed for other Kv channelopathies, for example, *KCNA1* mutations associated with episodic ataxia, for which mutations with dominant, recessive, and haploinsufficiency phenotypes have been documented (Adelman et al., 1995; Manganas et al., 2001a; Kullmann, 2002).

The cell type–specific differences in V378A trafficking are reminiscent of Kv2.1 expression in different neuronal subpopulations of the mammalian brain. For instance, Kv2.1 clusters colocalize with ryanodine receptor–rich calcium signaling domains at the plasma membrane to a different extent in striatal and neocortical neurons (Mandikian et al., 2014), and in cultured hippocampal interneurons versus principal neurons (Antonucci et al., 2001). Additionally, steady-state levels of Kv2.1 phosphorylation also differ between different

neuronal subpopulations (Mandikian et al., 2014). Cell type–specific differences in the subcellular localization of Kv2.1 channels are also observed in different heterologous cell backgrounds (Scannevin et al., 1996; Mohapatra and Trimmer, 2006). Our results suggest that expression and localization defects may contribute to the pathophysiological impact of disease-causing Kv2.1 mutations in a cell type–specific fashion. As Kv2.1 channel localization plays a structural role in neurons in contributing to the formation of plasma membrane–ER junctions and recruiting junctional proteins including those involved in intracellular Ca^{2+} signaling (Antonucci et al., 2001; Fox et al., 2015), changes in Kv2.1 localization could yield neurological consequences related to nonconducting functions of Kv2.1. The cell type–specific pharmacological rescue of the V378A variant indicates that effects on subcellular localization should be considered in therapeutic strategies targeting disease-causing Kv2.1 variants, as attempts to pharmacologically inhibit their aberrant depolarizing currents could inadvertently result in greater functional expression of disease-causing channels.

We thank the family of the patient for participation. This work is dedicated to the memory of coauthor Kenneth Sungjin Eum (1987–2014). Ken was a talented PhD student who conducted much of the electrophysiology. He was especially driven by this opportunity to study the mechanisms underlying debilitating disease.

We acknowledge support from the Clare Giannini Fund (to S.F. Kingsmore) and the NIH (award R01 NS042225 to J.S. Trimmer). GxTX was synthesized at the Molecular Foundry of the Lawrence Berkeley National Laboratory under US Department of Energy contract no. DE-AC02-05CH11231.

The authors declare no competing financial interests.

Author contributions: Conception and design of exome sequencing experiments: S.F. Kingsmore, N. Miller, C.J. Saunders, and E.G. Farrow. Analysis and interpretation of exome sequencing data: C.J. Saunders, E.G. Farrow, I. Thiffault, and N. Miller. Contributed reagents/materials/analysis tools: N. Miller and E.G. Farrow. Patient recruitment and clinical investigations: N.P. Safina, L. Grote, and S. Soden. Electrophysiology: K.S. Eum, D.C. Austin (performed), and J.T. Sack (directed). Molecular biology, cell biology, and biochemistry: D.J. Speca, M.M. Cobb (performed), and J.S. Trimmer (directed). Writing: I. Thiffault, C.J. Saunders, N.P. Safina, and L. Grote (sequencing and clinical); D.J. Speca, M.M. Cobb, and J.S. Trimmer (molecular biology, cell biology, and biochemistry); and J.T. Sack (electrophysiology).

Sharona E. Gordon served as editor.

Submitted: 26 May 2015
Accepted: 7 October 2015

REFERENCES

Adelman, J.P., C.T. Bond, M. Pessia, and J. Maylie. 1995. Episodic ataxia results from voltage-dependent potassium channels with altered functions. *Neuron.* 15:1449–1454. http://dx.doi.org/10.1016/0896-6273(95)90022-5

Adzhubei, I.A., S. Schmidt, L. Peshkin, V.E. Ramensky, A. Gerasimova, P. Bork, A.S. Kondrashov, and S.R. Sunyaev. 2010. A method and server for predicting damaging missense mutations. *Nat. Methods.* 7:248–249. http://dx.doi.org/10.1038/nmeth0410-248

Antonucci, D.E., S.T. Lim, S. Vassanelli, and J.S. Trimmer. 2001. Dynamic localization and clustering of dendritic Kv2.1 voltage-dependent potassium channels in developing hippocampal neurons. *Neuroscience.* 108:69–81. http://dx.doi.org/10.1016/S0306-4522(01)00476-6

Balijepalli, S.Y., C.L. Anderson, E.C. Lin, and C.T. January. 2010. Rescue of mutated cardiac ion channels in inherited arrhythmia syndromes. *J. Cardiovasc. Pharmacol.* 56:113–122. http://dx.doi.org/10.1097/FJC.0b013e3181dab014

Bell, C.J., D.L. Dinwiddie, N.A. Miller, S.L. Hateley, E.E. Ganusova, J. Mudge, R.J. Langley, L. Zhang, C.C. Lee, F.D. Schilkey, et al. 2011. Carrier testing for severe childhood recessive diseases by next-generation sequencing. *Sci. Transl. Med.* 3:65ra4. http://dx.doi.org/10.1126/scitranslmed.3001756

Berg, A.T., S.F. Berkovic, M.J. Brodie, J. Buchhalter, J.H. Cross, W. van Emde Boas, J. Engel, J. French, T.A. Glauser, G.W. Mathern, et al. 2010. Revised terminology and concepts for organization of seizures and epilepsies: Report of the ILAE Commission on Classification and Terminology, 2005–2009. *Epilepsia.* 51:676–685. http://dx.doi.org/10.1111/j.1528-1167.2010.02522.x

Cai, Z.W., J. Liu, H.Y. Li, and D.N. Sheppard. 2011. Targeting F508del-CFTR to develop rational new therapies for cystic fibrosis. *Acta Pharmacol. Sin.* 32:693–701. http://dx.doi.org/10.1038/aps.2011.71

Cavaretta, J.P., K.R. Sherer, K.Y. Lee, E.H. Kim, R.S. Issema, and H.J. Chung. 2014. Polarized axonal surface expression of neuronal KCNQ potassium channels is regulated by calmodulin interaction with KCNQ2 subunit. *PLoS One.* 9:e103655. http://dx.doi.org/10.1371/journal.pone.0103655

Covanis, A. 2014. Clinical management of epileptic encephalopathies of childhood and infancy. *Expert Rev. Neurother.* 14:687–701. http://dx.doi.org/10.1586/14737175.2014.919854

Dedek, K., L. Fusco, N. Teloy, and O.K. Steinlein. 2003. Neonatal convulsions and epileptic encephalopathy in an Italian family with a missense mutation in the fifth transmembrane region of KCNQ2. *Epilepsy Res.* 54:21–27. http://dx.doi.org/10.1016/S0920-1211(03)00037-8

Devaux, J.J., K.A. Kleopa, E.C. Cooper, and S.S. Scherer. 2004. KCNQ2 is a nodal K^+ channel. *J. Neurosci.* 24:1236–1244. http://dx.doi.org/10.1523/JNEUROSCI.4512-03.2004

Du, J., L.L. Haak, E. Phillips-Tansey, J.T. Russell, and C.J. McBain. 2000. Frequency-dependent regulation of rat hippocampal somato-dendritic excitability by the K^+ channel subunit Kv2.1. *J. Physiol.* 522:19–31. http://dx.doi.org/10.1111/j.1469-7793.2000.t01-2-00019.xm

Dyment, D.A., M. Tétreault, C.L. Beaulieu, T. Hartley, P. Ferreira, J.W. Chardon, J. Marcadier, S.L. Sawyer, S.J. Mosca, A.M. Innes, et al. 2015. Whole-exome sequencing broadens the phenotypic spectrum of rare pediatric epilepsy: a retrospective study. *Clin. Genet.* 88:34–40. http://dx.doi.org/10.1111/cge.12464

EuroEPINOMICS-RES. 2014. De novo mutations in synaptic transmission genes including DNM1 cause epileptic encephalopathies. *Am. J. Hum. Genet.* 95:360–370. http://dx.doi.org/10.1016/j.ajhg.2014.08.013

Fox, P.D., R.J. Loftus, and M.M. Tamkun. 2013. Regulation of Kv2.1 K^+ conductance by cell surface channel density. *J. Neurosci.* 33:1259–1270.http://dx.doi.org/10.1523/JNEUROSCI.3008-12.2013

Fox, P.D., C.J. Haberkorn, E.J. Akin, P.J. Seel, D. Krapf, and M.M. Tamkun. 2015. Induction of stable ER-plasma-membrane junctions by Kv2.1 potassium channels. *J. Cell Sci.* 128:2096–2105. http://dx.doi.org/10.1242/jcs.166009

Gagnier, J.J., G. Kienle, D.G. Altman, D. Moher, H. Sox, D. Riley, and CARE Group. 2013. The CARE guidelines: Consensus-based clinical case reporting guideline development. *Glob. Adv. Health Med.* 2:38–43. http://dx.doi.org/10.7453/gahmj.2013.008

Guan, D., T. Tkatch, D.J. Surmeier, W.E. Armstrong, and R.C. Foehring. 2007. Kv2 subunits underlie slowly inactivating potassium current in rat neocortical pyramidal neurons. *J. Physiol.* 581:941–960. http://dx.doi.org/10.1113/jphysiol.2007.128454

Gupta, K., M. Zamanian, C. Bae, M. Milescu, D. Krepkiy, D.C. Tilley, J.T. Sack, Y.Y. Vladimir, J.I. Kim, and K.J. Swartz. 2015. Tarantula toxins use common surfaces for interacting with Kv and ASIC ion channels. *eLife.* 4:e06774. http://dx.doi.org/10.7554/eLife.06774

Heginbotham, L., Z. Lu, T. Abramson, and R. MacKinnon. 1994. Mutations in the K^+ channel signature sequence. *Biophys. J.* 66:1061–1067. http://dx.doi.org/10.1016/S0006-3495(94)80887-2

Herrington, J., Y.P. Zhou, R.M. Bugianesi, P.M. Dulski, Y. Feng, V.A. Warren, M.M. Smith, M.G. Kohler, V.M. Garsky, M. Sanchez, et al. 2006. Blockers of the delayed-rectifier potassium current in pancreatic beta-cells enhance glucose-dependent insulin secretion. *Diabetes.* 55:1034–1042. http://dx.doi.org/10.2337/diabetes.55.04.06.db05-0788

Hsu, V.W., N. Shah, and R.D. Klausner. 1992. A brefeldin A-like phenotype is induced by the overexpression of a human ERD-2-like protein, ELP-1. *Cell.* 69:625–635. http://dx.doi.org/10.1016/0092-8674(92)90226-3

Ikeda, S.R., F. Soler, R.D. Zühlke, R.H. Joho, and D.L. Lewis. 1992. Heterologous expression of the human potassium channel Kv2.1 in clonal mammalian cells by direct cytoplasmic microinjection of cRNA. *Pflugers Arch.* 422:201–203. http://dx.doi.org/10.1007/BF00370422

King, A.N., C.F. Manning, and J.S. Trimmer. 2014. A unique ion channel clustering domain on the axon initial segment of mammalian neurons. *J. Comp. Neurol.* 522:2594–2608. http://dx.doi.org/10.1002/cne.23551

Kullmann, D.M. 2002. The neuronal channelopathies. *Brain.* 125:1177–1195. http://dx.doi.org/10.1093/brain/awf130

Kumar, P., S. Henikoff, and P.C. Ng. 2009. Predicting the effects of coding non-synonymous variants on protein function using the SIFT algorithm. *Nat. Protoc.* 4:1073–1081. http://dx.doi.org/10.1038/nprot.2009.86

Lalik, P.H., D.S. Krafte, W.A. Volberg, and R.B. Ciccarelli. 1993. Characterization of endogenous sodium channel gene expressed in Chinese hamster ovary cells. *Am. J. Physiol.* 264:C803–C809.

Leidenheimer, N.J., and K.G. Ryder. 2014. Pharmacological chaperoning: A primer on mechanism and pharmacology. *Pharmacol. Res.* 83:10–19. http://dx.doi.org/10.1016/j.phrs.2014.01.005

Li, X.N., J. Herrington, A. Petrov, L. Ge, G. Eiermann, Y. Xiong, M.V. Jensen, H.E. Hohmeier, C.B. Newgard, M.L. Garcia, et al. 2013. The role of voltage-gated potassium channels Kv2.1 and Kv2.2 in the regulation of insulin and somatostatin release from pancreatic islets. *J. Pharmacol. Exp. Ther.* 344:407–416. http://dx.doi.org/10.1124/jpet.112.199083

Lim, S.T., D.E. Antonucci, R.H. Scannevin, and J.S. Trimmer. 2000. A novel targeting signal for proximal clustering of the Kv2.1 K^+ channel in hippocampal neurons. *Neuron.* 25:385–397. http://dx.doi.org/10.1016/S0896-6273(00)80902-2

Liu, P.W., and B.P. Bean. 2014. Kv2 channel regulation of action potential repolarization and firing patterns in superior cervical ganglion neurons and hippocampal CA1 pyramidal neurons. *J. Neurosci.* 34:4991–5002. http://dx.doi.org/10.1523/JNEUROSCI.1925-13.2014

MacKinnon, R. 1991. Determination of the subunit stoichiometry of a voltage-activated potassium channel. *Nature.* 350:232–235. http://dx.doi.org/10.1038/350232a0

Malin, S.A., and J.M. Nerbonne. 2002. Delayed rectifier K^+ currents, IK, are encoded by Kv2 alpha-subunits and regulate tonic firing in mammalian sympathetic neurons. *J. Neurosci.* 22:10094–10105.

Maljevic, S., and H. Lerche. 2014. Potassium channel genes and benign familial neonatal epilepsy. *Prog. Brain Res.* 213:17–53. http://dx.doi.org/10.1016/B978-0-444-63326-2.00002-8

Mandikian, D., E. Bocksteins, L.K. Parajuli, H.I. Bishop, O. Cerda, R. Shigemoto, and J.S. Trimmer. 2014. Cell type-specific spatial and functional coupling between mammalian brain Kv2.1 K^+ channels and ryanodine receptors. *J. Comp. Neurol.* 522:3555–3574. http://dx.doi.org/10.1002/cne.23641

Manganas, L.N., and J.S. Trimmer. 2000. Subunit composition determines Kv1 potassium channel surface expression. *J. Biol. Chem.* 275:29685–29693. http://dx.doi.org/10.1074/jbc.M005010200

Manganas, L.N., S. Akhtar, D.E. Antonucci, C.R. Campomanes, J.O. Dolly, and J.S. Trimmer. 2001a. Episodic ataxia type-1 mutations in the Kv1.1 potassium channel display distinct folding and intracellular trafficking properties. *J. Biol. Chem.* 276:49427–49434. http://dx.doi.org/10.1074/jbc.M109325200

Manganas, L.N., Q. Wang, R.H. Scannevin, D.E. Antonucci, K.J. Rhodes, and J.S. Trimmer. 2001b. Identification of a trafficking determinant localized to the Kv1 potassium channel pore. *Proc. Natl. Acad. Sci. USA.* 98:14055–14059. http://dx.doi.org/10.1073/pnas.241403898

Milescu, M., F. Bosmans, S. Lee, A.A. Alabi, J.I. Kim, and K.J. Swartz. 2009. Interactions between lipids and voltage sensor paddles detected with tarantula toxins. *Nat. Struct. Mol. Biol.* 16:1080–1085. http://dx.doi.org/10.1038/nsmb.1679

Misonou, H., D.P. Mohapatra, E.W. Park, V. Leung, D. Zhen, K. Misonou, A.E. Anderson, and J.S. Trimmer. 2004. Regulation of ion channel localization and phosphorylation by neuronal activity. *Nat. Neurosci.* 7:711–718. http://dx.doi.org/10.1038/nn1260

Misonou, H., S.M. Thompson, and X. Cai. 2008. Dynamic regulation of the Kv2.1 voltage-gated potassium channel during brain ischemia through neuroglial interaction. *J. Neurosci.* 28:8529–8538. http://dx.doi.org/10.1523/JNEUROSCI.1417-08.2008

Mohapatra, D.P., and J.S. Trimmer. 2006. The Kv2.1 C terminus can autonomously transfer Kv2.1-like phosphorylation-dependent localization, voltage-dependent gating, and muscarinic modulation to diverse Kv channels. *J. Neurosci.* 26:685–695. http://dx.doi.org/10.1523/JNEUROSCI.4620-05.2006

Murakoshi, H., and J.S. Trimmer. 1999. Identification of the Kv2.1 K^+ channel as a major component of the delayed rectifier K^+ current in rat hippocampal neurons. *J. Neurosci.* 19:1728–1735.

Nabbout, R., and O. Dulac. 2012. Epilepsy: Genetics of early-onset epilepsy with encephalopathy. *Nat. Rev. Neurol.* 8:129–130. http://dx.doi.org/10.1038/nrneurol.2012.12

O'Connell, K.M., R. Loftus, and M.M. Tamkun. 2010. Localization-dependent activity of the Kv2.1 delayed-rectifier K^+ channel. *Proc. Natl. Acad. Sci. USA.* 107:12351–12356. http://dx.doi.org/10.1073/pnas.1003028107

Parcej, D.N., and J.O. Dolly. 1989. Dendrotoxin acceptor from bovine synaptic plasma membranes. Binding properties, purification and subunit composition of a putative constituent of certain voltage-activated K^+ channels. *Biochem. J.* 257:899–903. http://dx.doi.org/10.1042/bj2570899

Rangaraju, S., K.K. Khoo, Z.P. Feng, G. Crossley, D. Nugent, I. Khaytin, V. Chi, C. Pham, P. Calabresi, M.W. Pennington, et al. 2010. Potassium channel modulation by a toxin domain in matrix metalloprotease 23. *J. Biol. Chem.* 285:9124–9136. http://dx.doi.org/10.1074/jbc.M109.071266

Richards, C.S., S. Bale, D.B. Bellissimo, S. Das, W.W. Grody, M.R. Hegde, E. Lyon, and B.E. Ward. 2008. ACMG recommendations for standards for interpretation and reporting of sequence variations: Revisions 2007. *Genet. Med.* 10:294–300. http://dx.doi.org/10.1097/GIM.0b013e31816b5cae

Ridgway, N.D., P.A. Dawson, Y.K. Ho, M.S. Brown, and J.L. Goldstein. 1992. Translocation of oxysterol binding protein to Golgi apparatus triggered by ligand binding. *J. Cell Biol.* 116:307–319. http://dx.doi.org/10.1083/jcb.116.2.307

Ruppersberg, J.P., K.H. Schröter, B. Sakmann, M. Stocker, S. Sewing, and O. Pongs. 1990. Heteromultimeric channels formed by rat brain potassium-channel proteins. *Nature.* 345:535–537. http://dx.doi.org/10.1038/345535a0

Sack, J.T., R.W. Aldrich, and W.F. Gilly. 2004. A gastropod toxin selectively slows early transitions in the Shaker K channel's activation pathway. *J. Gen. Physiol.* 123:685–696. http://dx.doi.org/10.1085/jgp.200409047

Sack, J.T., O. Shamotienko, and J.O. Dolly. 2008. How to validate a heteromeric ion channel drug target: Assessing proper expression of concatenated subunits. *J. Gen. Physiol.* 131:415–420. http://dx.doi.org/10.1085/jgp.200709939

Sarmiere, P.D., C.M. Weigle, and M.M. Tamkun. 2008. The Kv2.1 K^+ channel targets to the axon initial segment of hippocampal and cortical neurons in culture and in situ. *BMC Neurosci.* 9:112. http://dx.doi.org/10.1186/1471-2202-9-112

Saunders, C.J., N.A. Miller, S.E. Soden, D.L. Dinwiddie, A. Noll, N.A. Alnadi, N. Andraws, M.L. Patterson, L.A. Krivohlavek, J. Fellis, et al. 2012. Rapid whole-genome sequencing for genetic disease diagnosis in neonatal intensive care units. *Sci. Transl. Med.* 4:154ra135. http://dx.doi.org/10.1126/scitranslmed.3004041

Scannevin, R.H., H. Murakoshi, K.J. Rhodes, and J.S. Trimmer. 1996. Identification of a cytoplasmic domain important in the polarized expression and clustering of the Kv2.1 K^+ channel. *J. Cell Biol.* 135:1619–1632. http://dx.doi.org/10.1083/jcb.135.6.1619

Shi, G., A.K. Kleinklaus, N.V. Marrion, and J.S. Trimmer. 1994. Properties of Kv2.1 K^+ channels expressed in transfected mammalian cells. *J. Biol. Chem.* 269:23204–23211.

Singh, N.A., C. Charlier, D. Stauffer, B.R. DuPont, R.J. Leach, R. Melis, G.M. Ronen, I. Bjerre, T. Quattlebaum, J.V. Murphy, et al. 1998. A novel potassium channel gene, KCNQ2, is mutated in an inherited epilepsy of newborns. *Nat. Genet.* 18:25–29. http://dx.doi.org/10.1038/ng0198-25

Speca, D.J., G. Ogata, D. Mandikian, H.I. Bishop, S.W. Wiler, K. Eum, H.J. Wenzel, E.T. Doisy, L. Matt, K.L. Campi, et al. 2014. Deletion of the Kv2.1 delayed rectifier potassium channel leads to neuronal and behavioral hyperexcitability. *Genes Brain Behav.* 13:394–408. http://dx.doi.org/10.1111/gbb.12120

Srivastava, S., J.S. Cohen, H. Vernon, K. Barañano, R. McClellan, L. Jamal, S. Naidu, and A. Fatemi. 2014. Clinical whole exome sequencing in child neurology practice. *Ann. Neurol.* 76:473–483. http://dx.doi.org/10.1002/ana.24251

Tanaka, M., and W. Herr. 1990. Differential transcriptional activation by Oct-1 and Oct-2: Interdependent activation domains induce Oct-2 phosphorylation. *Cell.* 60:375–386. http://dx.doi.org/10.1016/0092-8674(90)90589-7

Tilley, D.C., K.S. Eum, S. Fletcher-Taylor, D.C. Austin, C. Dupré, L.A. Patrón, R.L. Garcia, K. Lam, V. Yarov-Yarovoy, B.E. Cohen, and J.T. Sack. 2014. Chemoselective tarantula toxins report voltage activation of wild-type ion channels in live cells. *Proc. Natl. Acad. Sci. USA.* 111:E4789–E4796. http://dx.doi.org/10.1073/pnas.1406876111

Torkamani, A., K. Bersell, B.S. Jorge, R.L. Bjork Jr., J.R. Friedman, C.S. Bloss, J. Cohen, S. Gupta, S. Naidu, C.G. Vanoye, et al. 2014. De novo KCNB1 mutations in epileptic encephalopathy. *Ann. Neurol.* 76:529–540. http://dx.doi.org/10.1002/ana.24263

Trimmer, J.S. 1991. Immunological identification and characterization of a delayed rectifier K^+ channel polypeptide in rat brain. *Proc. Natl. Acad. Sci. USA.* 88:10764–10768. http://dx.doi.org/10.1073/pnas.88.23.10764

Trimmer, J.S. 2015. Subcellular localization of K^+ channels in mammalian brain neurons: Remarkable precision in the midst of extraordinary complexity. *Neuron.* 85:238–256. http://dx.doi.org/10.1016/j.neuron.2014.12.042

Vacher, H., D.P. Mohapatra, H. Misonou, and J.S. Trimmer. 2007. Regulation of Kv1 channel trafficking by the mamba snake neurotoxin dendrotoxin K. *FASEB J.* 21:906–914. http://dx.doi.org/10.1096/fj.06-7229com

Weckhuysen, S., S. Mandelstam, A. Suls, D. Audenaert, T. Deconinck, L.R. Claes, L. Deprez, K. Smets, D. Hristova, I. Yordanova, et al. 2012. KCNQ2 encephalopathy: Emerging phenotype of a neonatal epileptic encephalopathy. *Ann. Neurol.* 71:15–25. http://dx.doi.org/10.1002/ana.22644

Weckhuysen, S., V. Ivanovic, R. Hendrickx, R. Van Coster, H. Hjalgrim, R.S. Møller, S. Grønborg, A.S. Schoonjans, B. Ceulemans, S.B. Heavin, et al. 2013. Extending the *KCNQ2* encephalopathy spectrum: Clinical and neuroimaging findings in 17 patients. *Neurology.* 81:1697–1703. http://dx.doi.org/10.1212/01.wnl.0000435296.72400.a1

Wimmer, V.C., C.A. Reid, E.Y. So, S.F. Berkovic, and S. Petrou. 2010. Axon initial segment dysfunction in epilepsy. *J. Physiol.* 588:1829–1840. http://dx.doi.org/10.1113/jphysiol.2010.188417

Zhang, Z.H., Y.T. Lee, K. Rhodes, K. Wang, T.M. Argentieri, and Q. Wang. 2003. Inhibitory effects of pimozide on cloned and native voltage-gated potassium channels. *Brain Res. Mol. Brain Res.* 115:29–38. http://dx.doi.org/10.1016/S0169-328X(03)00175-X

Zhou, Y., J.H. Morais-Cabral, A. Kaufman, and R. MacKinnon. 2001. Chemistry of ion coordination and hydration revealed by a K^+ channel-Fab complex at 2.0 Å resolution. *Nature.* 414:43–48. http://dx.doi.org/10.1038/35102009